

Supplementary Materials

ATR blockade potentiates the effects of genotoxic agents in vitro and promotes antitumor immunity in a mouse model of Non-Small Cell Lung Cancer

Mavroeidi et al.

Table of contents

Figure S1. Representative dot plots showing gating strategy for identifying T cell populations from single cell suspensions from tumors.

Figure S2. Sensitivity of lung cancer cell lines following treatment with AZD6738, and/or genotoxic agents.

Figure S3. DDR parameters following treatment with UVC and/or AZD6738.

Figure S4. ATR inhibition combined with chemotherapy treatment of lung cancer in vivo.

Figure S5. Flow cytometry analysis for T cell populations isolated from single cell suspensions from spleens.

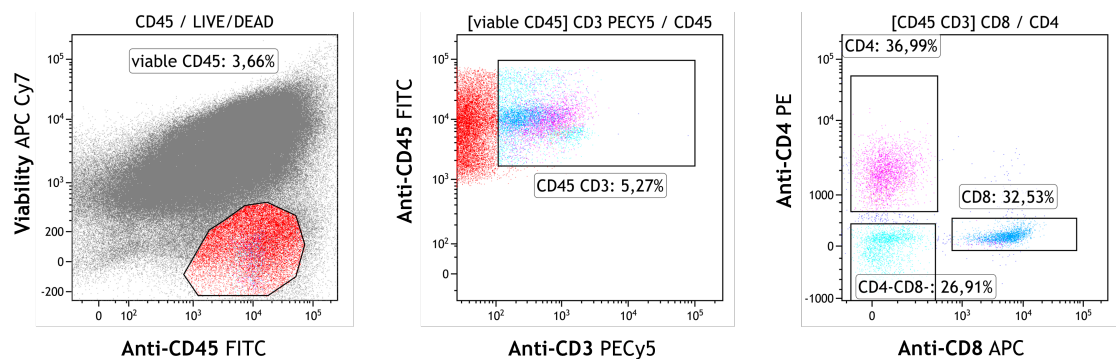


Figure S1. Representative dot plots showing gating strategy for identifying T cell populations from single cell suspensions from tumors

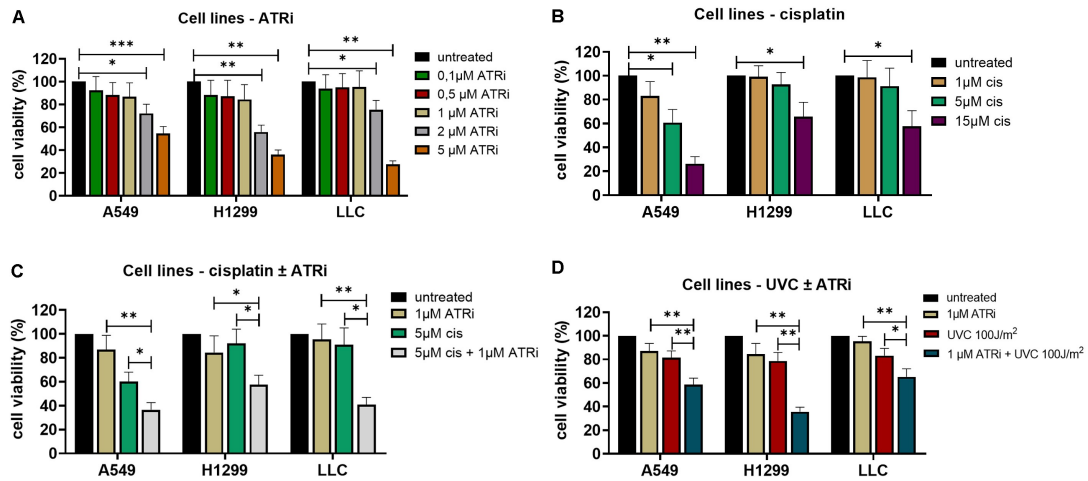


Figure S2. Sensitivity of lung cancer cell lines following treatment with AZD6738, and/or genotoxic agents. Cell viability was assessed by SRB assay after treatment with (A) AZD6738-only, (B) cisplatin-only, (C) combined treatment with cisplatin and AZD6738, and (D) combined treatment with UVC and AZD6738. AZD6738 and cisplatin were administered concurrently for 72 h. For UVC irradiation experiments, cells were pretreated with AZD6738 for 72 h, followed by UVC exposure and collected 6hrs after irradiation. Values were normalized to internal controls and are presented as percentage. Each experiment was performed at least three independent times. Error bars represent SD.

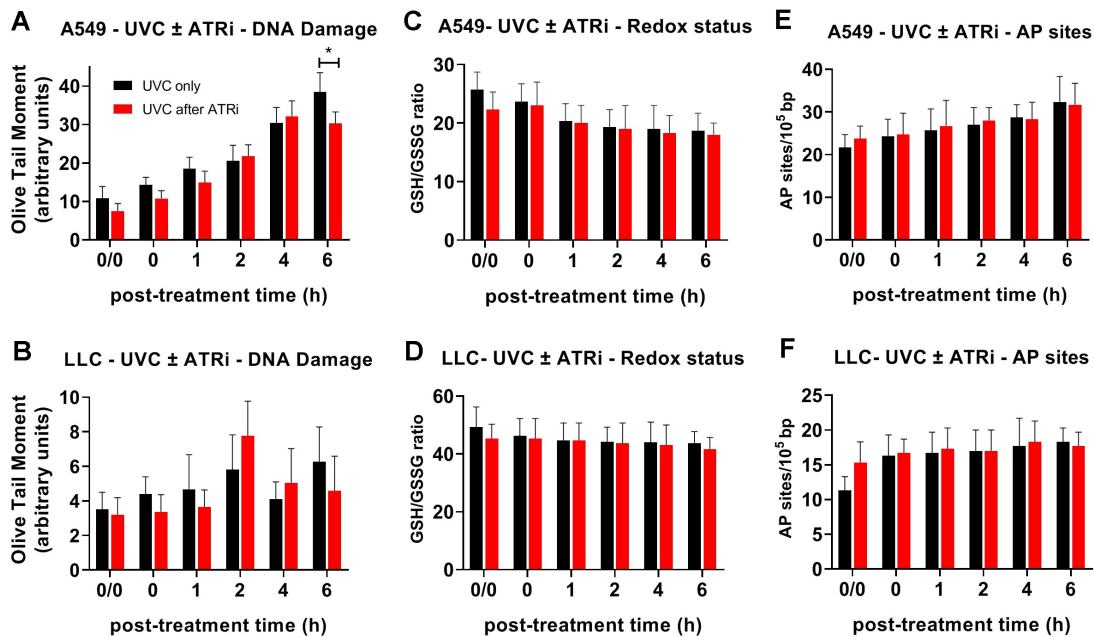


Figure S3. DDR parameters following treatment with UVC and/or AZD6738. The kinetics of DNA damage formation/repair in A549 (A), and LLC (B) cell lines, measured with alkaline comet assay. The kinetics of redox status in A549 (C), and LLC (D) cell lines, as well as the AP-sites formation/repair in A549 (E) and LLC (F) cell lines are presented. Error bars represent SD; * $p < 0.05$.

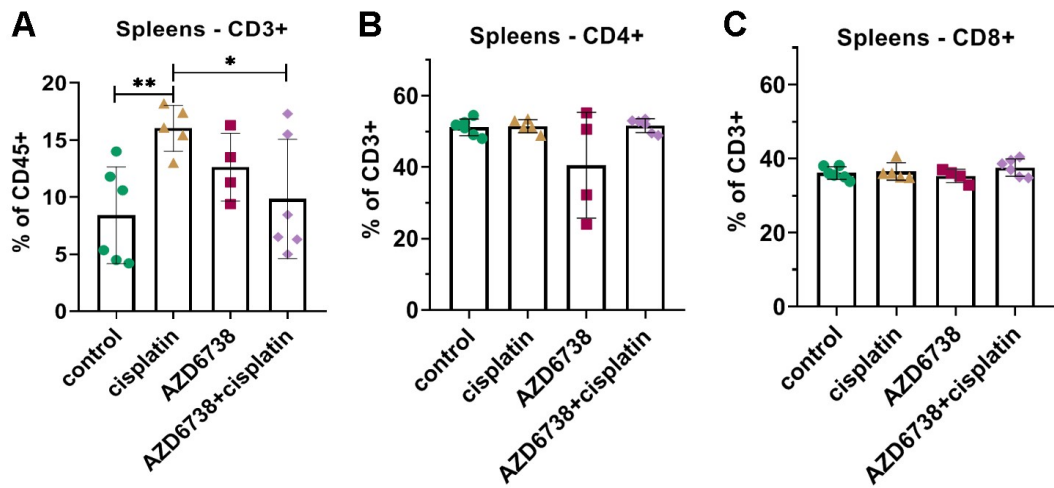


Figure S4. ATR inhibition combined with chemotherapy treatment of lung cancer in vivo. (A) CD3⁺ cells representing the total T cell population in spleens isolated from mice, (B) CD4⁺ T helper cells. (C) CD8⁺ T cytotoxic cells within the T cell compartment in spleens.

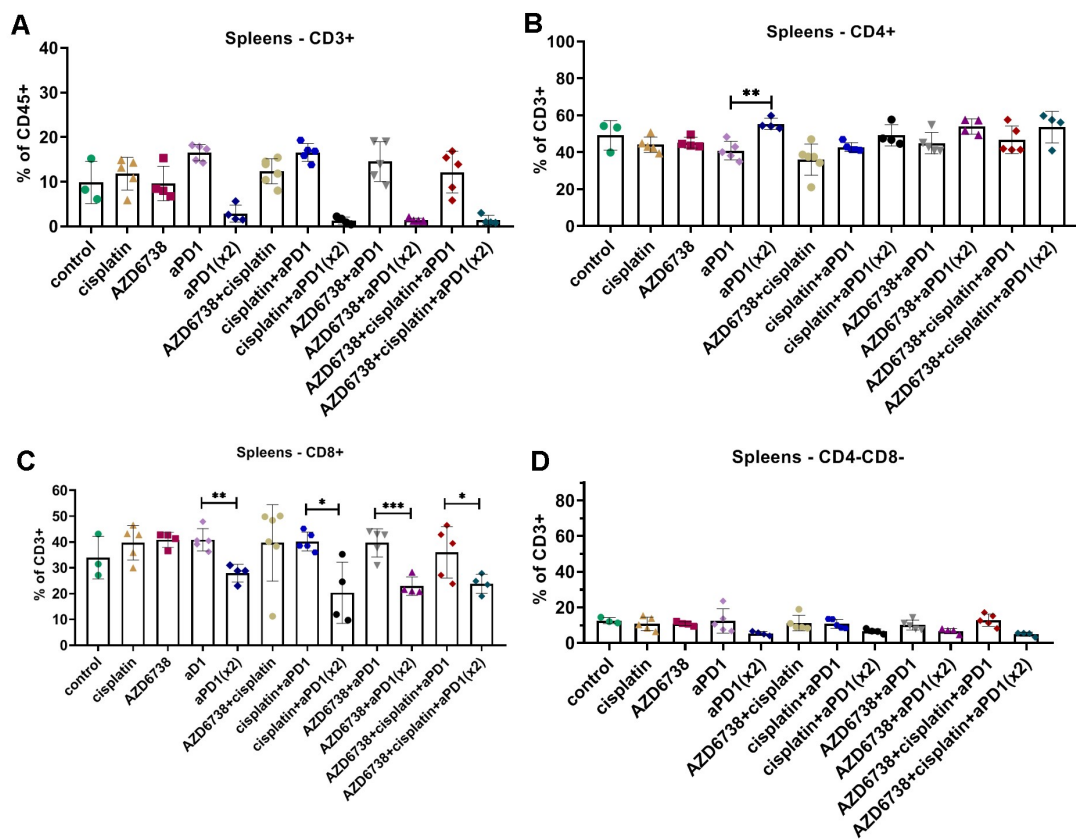


Figure S5. Flow cytometry analysis for T cell populations isolated from single cell suspensions from spleens. (A) CD3⁺ cells representing the total T cell population in spleens. (B) CD4⁺ T helper cells, (C) CD8⁺ T cytotoxic cells, and (D) Double negative (CD4⁻CD8⁻) T cells shown as proportion of the CD3⁺ population.